

# The Magnetic Layer in Powder River and Denver-Julesburg basins: a new crustal temperature constraint for estimating thermal properties in sedimentary basins

Dale E. Bird\*, Bird Geophysical; William E. Cathey, Earthfield Technology, LLC; Naila Dowla, Consultant

## Summary

The Earth's magnetic field, after core correction, is dominated by anomalies produced between crystalline basement and Curie point depth horizons, or The Magnetic Layer (TML). Motivated by the idea that Curie point depth is also a temperature horizon (~580°C where cooling iron becomes magnetic), we present a new method to integrate basement terrane and high-resolution magnetic basement depth interpretations with open-file station and well data to map thermal properties in sedimentary basins and TML, including temperature, thermal gradient, thermal conductivity, heat flow, heat production, and heat production layer thickness.

## Geology

The Powder River and Denver-Julesburg basins formed along the eastern perimeter of the Laramide deformation front (Figure 1) (DeCelles, 2004). The shape of these foreland basins is typically asymmetric with deeper parts in the western half – up to about six and four km respectively for Powder River and Denver-Julesburg. The Powder River Basin sits on Archean (> 2.5 Ga) basement rocks of the Wyoming terrane province, where even Hadean (~3.85 Ga) zircons have been recovered (Beartooth Mountains, Maier et al., 2012). Basement beneath the Denver-Julesburg Basin is a more complex amalgamation that includes late Paleoproterozoic juvenile oceanic arcs (Yavapai terrane province, ~1.76-1.72 Ga) and granitic intrusions (~1.72-1.68 Ga) (Whitmeyer and Karlstrom, 2007).

## Data

Except for the detailed basement depth interpretation, we use open-file thermal data from stations and wells, magnetic anomaly and Curie point depth grids, and a basement terrane interpretation. Measured temperature, heat flow, thermal conductivity and heat production values are available from Southern Methodist University (SMU) Geothermal Lab and AAPG Datapages, Inc. (Jessop et al., 1976; Blackwell et al., 2011). Additional heat production data were recently compiled (Hasterok and Webb, 2017). Magnetic, Curie point, and surface temperature grids are described by Finn et al. (2001), Li et al. (2017), and Matsuura and Wilmot (2018), respectively. Whitmeyer and Karlstrom (2007) integrated outcrop, well and magnetic data to produce a basement terrane map of North America (Figure 1c).

## Methods

Inverted magnetic susceptibilities in TML (Figure 1b), derived from a 3D model, are used to modify Whitmeyer and Karlstrom's (2007) terrane map. Basement morphology, TML geometry, and modified basement terranes control thermal calculations based on two fundamental heat flow equations (Turcotte and Shubert, 2002) and an empirical relation:

(1)  $Q = k \cdot dT/dZ$  where  $Q$  is heat flow,  $k$  is thermal conductivity,  $T$  is temperature, and  $Z$  is depth;

(2)  $Q_{TOT} = Q_{BG} + A_0D$  where  $Q_{TOT}$  is total heat flow,  $Q_{BG}$  is background heat flow,  $A_0$  is heat produced from continental TML, and  $D$  is heat producing layer thickness in TML; and

Global experiment (Pollack and Chapman, 1977): on average,  $Q_{BG}$  is 60% of  $Q_{TOT}$ , and  $A_0D$  is 40% of  $Q_{TOT}$ .

## Results

The basic heat flow equation (1), or Fourier's Law, is simply a geothermal gradient scaled by thermal conductivity. We determine basin and TML thermal gradients between three temperature horizons: near surface, basement and Curie point. The near surface horizon is calculated using surface and bottom hole temperatures. Heat flow stations are used to calculate basement temperature. After correcting for heat produced within the basin (Souche et al., 2017), background and TML heat flow are estimated from Pollack and Chapman's (1977) relation. Finally, equation (1) is used again to calculate TML thermal conductivity, and equation (2) is used to calculate the thickness of the heat producing layer in TML.

## Conclusions

Globally, Curie point depths essentially track the base of the crust (Moho), although they are generally a little shallower beneath continents and a little deeper beneath oceans. Therefore, in addition to thermal properties in sedimentary basins, the method described above also quantifies deeper thermal properties in the crystalline crust (The Magnetic Layer): temperature, thermal gradient, thermal conductivity, heat flow, heat production, and heat production layer thickness. Furthermore, interpreted basement depths and terranes, as well as inferred heat production levels, may be integrated in basin model studies. Our new method may be applied anywhere – the workflow has been successfully employed in the Permian Basin and other areas world-wide.

## The Magnetic Layer

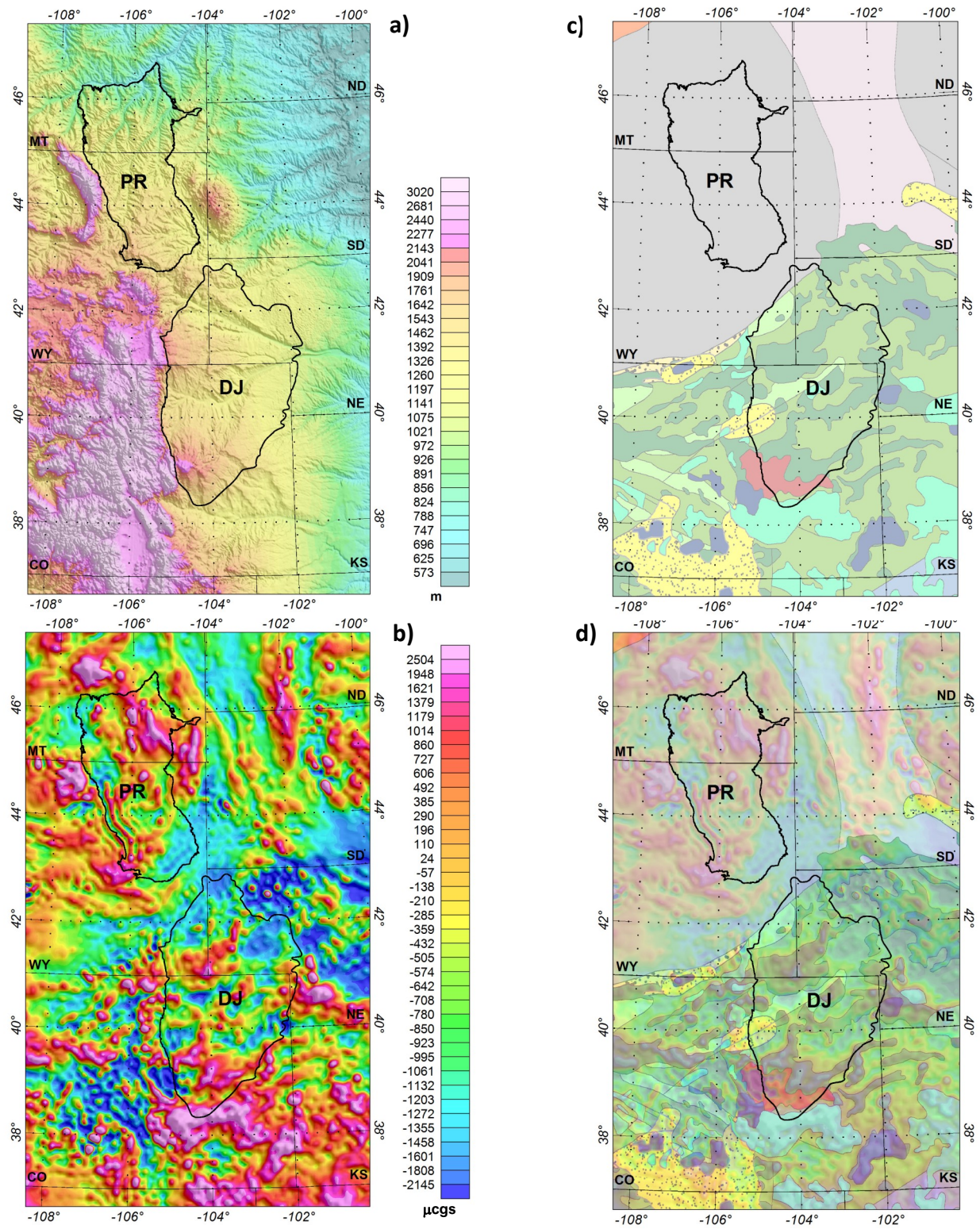


Figure 1: Powder River (PR) and Denver-Julesburg (DJ) basin outlines (heavy black): a) topography, b) inverted magnetic susceptibility, c) basement terranes (Whitmeyer and Karlstrom, 2007), d) transparency of basement terranes over inverted magnetic susceptibility.

*Bird, Cathey, and Dowla, The Magnetic Layer*

**References**

- Blackwell, D., Richards, M., Frone, Z., Batir, J., Ruzo, A., et al., 2011, Temperature at depth maps for the conterminous US and geothermal resource estimates: Geothermal Resources Council, Transactions, **35** (GRC1029452).
- DeCelles, P. G., 2004, Late Jurassic to Eocene evolution of the cordilleran thrust belt and foreland basin system, western U.S.A.: American Journal of Science, **304**, 105-168.
- Finn, C. A., Pilkington, M., Cuevas, A., Hernandez, I., and Urrutia, J., 2001, New digital magnetic anomaly database for North America: The Leading Edge, **20**, 870-872.
- Hasterok, D., and Webb, J., 2017, On the radiogenic heat production of igneous rocks: Geoscience Frontiers, **8**, 5, 919-940.
- Jessop, A. M., Hobart, M. A., and Sclater, J. G., 1976, The world heat flow data collection – 1975: Energy, Mines and Resources Canada, Earth Physics Branch, Geothermal Series, **5**, 10 p.
- Li, C. -F., Lu, Y., and Wang, J., 2017, A global reference model of Curie-point depths based on EMAG2: Scientific Reports, **7**, 1-9.
- Maier, A. C., Cates, N. L., Trail, D., and Mojzsis, S. J., 2012, Geology, age and field relations of Hadean zircon-bearing supracrustal rocks from Quad Creek, eastern Beartooth Mountains (Montana and Wyoming, USA): Chemical Geology, **312-313**, 47-57.
- Matsuura, K., and Wilmott, C. J., 2018, Terrestrial air temperature: 1900-2017 gridded monthly time series (v. 5.01): University of Delaware, Department of Geography.
- Pollack, H. N., and Chapman, D. S., 1977, Mantle heat flow: Earth and Planetary Science Letters, **34**, 174-184.
- Souche, A., Schmid, D. W., and Rupke, L., 2017, Interrelation between surface and basement heat flow in sedimentary basins: American Association of Petroleum Geologists Bulletin, **101**, 1697-1713.
- Turcotte, D. L., and Shubert, G., 2002, Geodynamics, second edition: Cambridge University Press.
- Whitmeyer, S. J., and Karlstrom, K. E., 2007, Tectonic model for the Proterozoic growth of North America: Geosphere, **3**, 220-259.

**Citation:** Bird, D. E., Cathey, W. E., and Dowla, N., 2022, The Magnetic Layer in Powder River and Denver-Julesburg basins: a new crustal temperature constraint for estimating thermal properties in sedimentary basins: American Association of Petroleum Geologists & Society of Exploration Geophysicists, International Meeting for Applied Geoscience & Energy (IMAGE), NEF 2, 2 p.